SUPPORTING INFORMATION

Thermal evaporation-oxidation deposited aluminum oxide as an interfacial modifier to improve the performance and stability of zinc oxide based planar perovskite solar cells.

*Carlos A. Rodríguez-Castañeda**,†* *Paola M. Moreno-Romero*†, *Asiel N. Corpus-Mendoza*†,§, *Guillermo Suarez-Campos*‡, *Margarita Miranda-Hernández*†, *Merida Sotelo-Lerma*‡, *Hailin* Hu**,†

†*Instituto de Energías Renovables – Universidad Nacional Autónoma de México, Priv. Xochicalco S/N, Temixco, Morelos, 62580, México.*
§*CONACYT - Universidad Nacional Autónoma de México, 62580 Temixco, Morelos, Mexico*
‡*Departamento de Investigación en Polímeros y Materiales, Universidad de Sonora, Blvd. Luis Encinas y Rosales s/n, Hermosillo, Sonora C.P. 83000, México*

Corresponding Authors: **carc@ier.unam.mx*, ***hzh@ier.unam.mx*

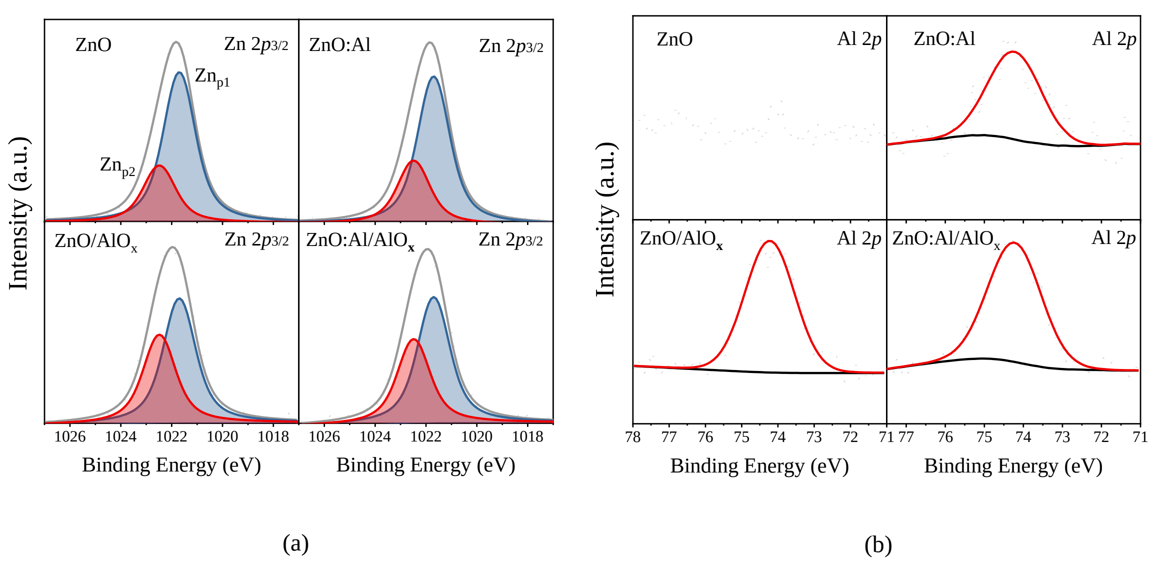

Figure S1. High resolution XPS spectra at (a) Zn $2p_{3/2}$ and (b) Al 2*p* binding energy regions of the surface of the four ZnO films.

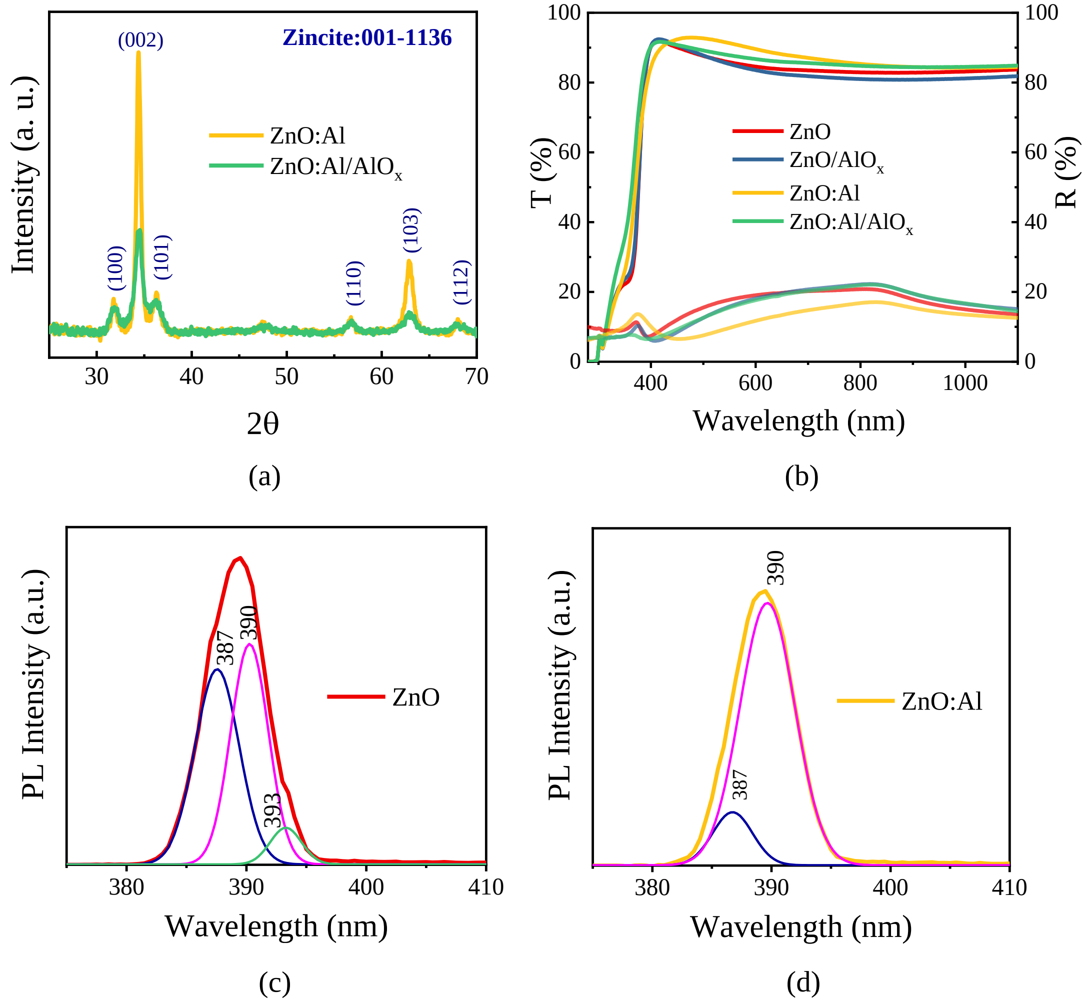

Figure S2. (a) XRD patterns of ZnO:Al and ZnO:Al/AlO_x films. (b) Transmittance (T) and reflectance (R) spectra of the four types of ZnO films. (c) Photoluminescence spectrum of ZnO thin film. (d) Photoluminescence spectrum of ZnO:Al thin film.

Using the transmittance (T) and reflectance (R) spectra and thickness (d) values, the absorption coefficient (α) spectra of ZnO films are calculated by using the following equation [S1]:

$$\alpha = -\frac{1}{d} ln\left(\frac{-(1-R)^2+\sqrt{(1-R)^4+4T^2R^2}}{2TR^2}\right) \tag{1}$$

The electrical properties of ZnO films are determined through the following relations [S1]:

Resistance R:

$$R = \frac{V}{I} \tag{2}$$

Resistivity ρ:

$$\rho = R \cdot \frac{w \cdot t}{L} \tag{3}$$

In Eq.2 and 3, the unit of R is Ohms, that of the current I is in Ampere, V is the applied voltage of the sample in Volts. In Eq.3, ρ is the resistivity, w is the electrode length, t is the film thickness and L is the separation between the two parallel electrodes. The conductivity σ of ZnO films is calculated as follows:

$$\sigma = \frac{1}{\rho} \tag{4}$$

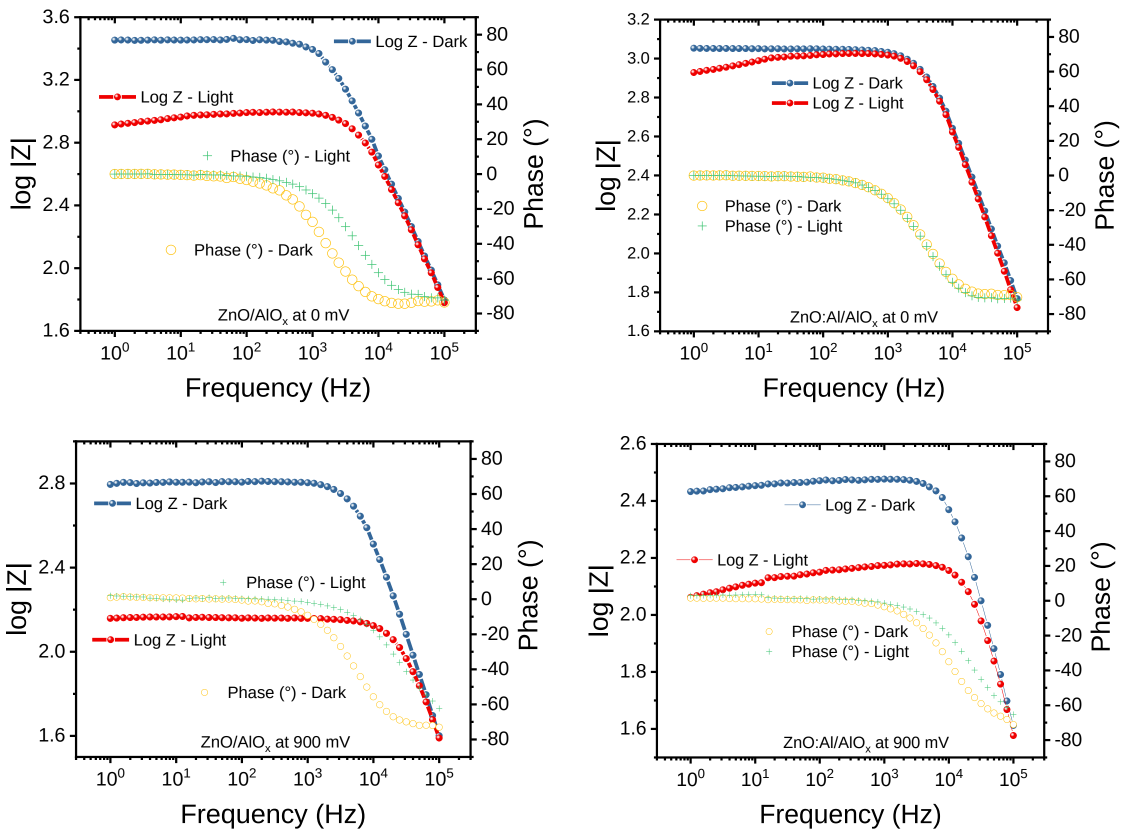

Figure S3. Bode diagrams at 0 V in dark and under illumination, at 900 mV in dark and under illumination of ZnO/AlO_x and $ZnO:Al/AlO_x$ samples.

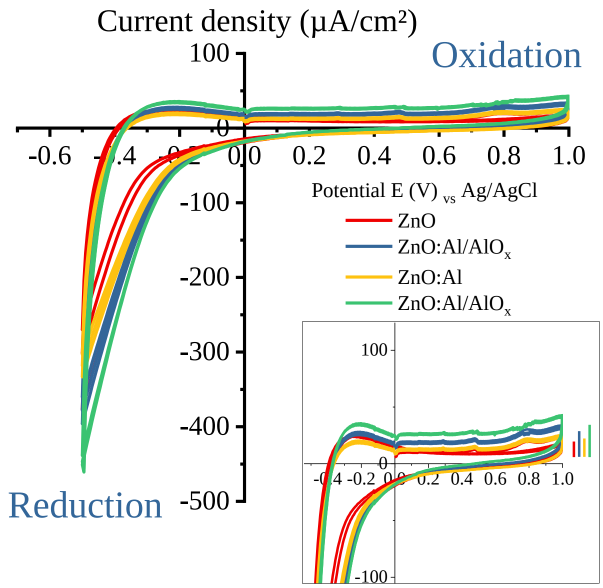

Figure S4. Cyclic voltammetry (CV) curves of the four ZnO samples in an electrolyte of 0.1 M $(CH_3CH_2CH_2CH_2)_4N(PF_6)$ in acetonitrile.

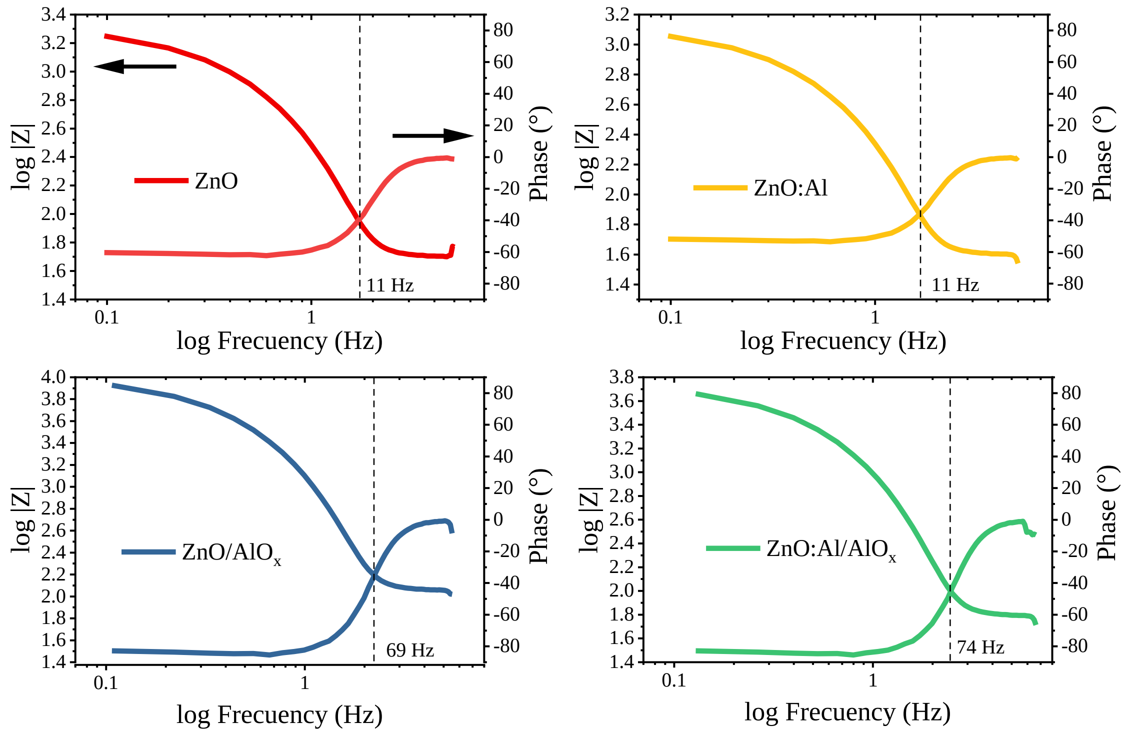

Figure S5. Electrochemical impedance spectroscopy measurements of the four ZnO samples.

Calculation for $\boldsymbol{E_C - E_F}$:

For a n-type semiconductor, the Fermi level E_F can be described as:

$$E_F = E_{F0} + k_B T ln\left(\frac{N_D}{N_i}\right), \tag{5}$$

where E_{F0} and N_i is the Fermi level and impurity concentration of the intrinsic semiconductor, respectively, k is the Boltzmann constant and T the absolute temperature. It is evident that for each type of semiconductor at the same temperature, its Fermi level depends on the concentration of dopant, N_D. It is reported that polycrystalline ZnO thin films prepared by atomic layer deposition with an N_D of about 10^{18} cm^{-3} give a difference between the conduction band edge (E_C) and Fermi level (we will call it as E_{F18}) of about 0.04 eV at room temperature [S2]. By using Eq.5,

$$E_C - E_{F18} = 0.04\ (eV) = E_C - \left\{E_{F0} + kT\ ln\left(\frac{10^{18}}{N_i}\right)\right\}. \tag{6}$$

Considering that:

$$ln\left(\frac{10^{18}}{N_i}\right) = ln\left(\frac{10^{17}}{N_i}\right) + ln(10) = ln\left(\frac{10^{16}}{N_i}\right) + ln(10^2), \tag{7}$$

we can estimate the $E_C - E_F$ values of the four types of ZnO by assuming that the N_i value is independent on the ZnO preparation process. The obtained values are listed in Table S1 by using the following deduction:

$$\begin{aligned}
0.04 &= E_C - \left\{E_{F0} + kT\ ln\left(\frac{10^{18}}{N_i}\right)\right\} \\
&= E_C - \left\{E_{F0} + kT\ \left\{ln\left(\frac{9.109\times10^{16}}{N_i}\right) + ln(10.978)\right\}\right\} = E_C - E_{F,ZnO} - 0.062 \\
&= E_C - \left\{E_{F0} + kT\ \left\{ln\left(\frac{7.621\times10^{16}}{N_i}\right) + ln(13.122)\right\}\right\} = E_C - E_{F,ZnO/AlOx} - 0.066 \\
&= E_C - \left\{E_{F0} + kT\ \left\{ln\left(\frac{1.093\times10^{17}}{N_i}\right) + ln(9.148)\right\}\right\} = E_C - E_{F,ZnO:Al} - 0.057
\end{aligned}$$

$$= E_C - \left\{E_{F0} + kT\left\{ln\left(\frac{7.128\times10^{16}}{N_i}\right) + ln(14.029)\right\}\right\} = E_C - E_{F,ZnO:al/AlOx} - 0.068$$

Consequently,

$$E_C - E_{F,ZnO} = 0.102\ eV$$
$$E_C - E_{F,ZnO/AlOx} = 0.106\ eV$$
$$E_C - E_{F,ZnO:Al} = 0.097\ eV$$
$$E_C - E_{F,ZnO:al/AlOx} = 0.108\ eV$$

Table S1. Flat-band, charge carrier concentration and electronic levels of ZnO, ZnO/AlO_x, ZnO:Al and ZnO:Al/AlO_x films.

Sample	**$V_{FB(Ag/AgCl)}$ (V)***	**N_D (cm^{-3})***	**E_F (eV)**	**$E_C - E_F$ (eV)**	**E_C (eV)**	**E_V (eV)**
ZnO	0.165	$9.109x10^{16}$	-4.58	0.10	-4.48	-7.62
ZnO/AlO_x	0.079	$7.621x10^{16}$	-4.49	0.11	-4.38	-7.52
ZnO:Al	0.146	$1.093x10^{17}$	-4.56	0.10	-4.46	-7.62
ZnO:Al/AlO_x	0.057	$7.128x10^{16}$	-4.47	0.11	-4.36	-7.52

*$V_{FB(Fc/Fc+)} = V_{FB(Ag/AgCl)}$ - 0.68V; $E_F = -5.1 - eV_{FB(Fc/Fc+)}$; $E_V = E_C - E_g$ (3.14 or 3.16 eV)

*$N_D= (2/(\varepsilon\ \varepsilon_0\ A^2 e\ (slope))\ (V-V_{FB}- kT/e)$

*ε = 8 to 10.9, depending on the range frequency measurement and film deposition process of ZnO [S3-S6].

The hysteresis phenomenon in a solar cell can be quantified with the hysteresis index (*HI*), defined as follows [S7]:

$$HI = \frac{\int_0^{V_{OC}} J_{(r)}\mathrm{d}V - \int_0^{V_{OC}} J_{(f)} dV}{\int_0^{V_{OC}} J_{(r)}\ dV}\ \mathrm{x}\ 100\%, \quad (13)$$

where $J_{(r)}$ is the current density measured in the reverse direction, and $J_{(f)}$, the current density measured at forward direction.

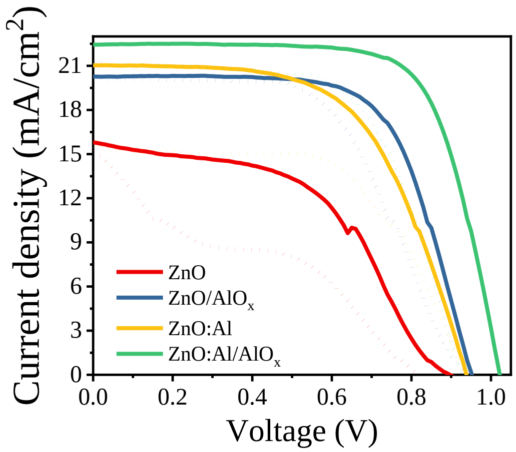

Sample	$\int_0^{Voc} J(r)$	$\int_0^{Voc} J(f)$	**HI (%)**	PCE (%) Forward	PCE (%) Reverse
ZnO	10.19	6.45	36.68	4.06	6.46
ZnO/AlO$_x$	16.77	14.96	10.79	10.74	12.07
ZnO:Al	16.33	11.96	19.79	8.75	10.47
ZnO:Al/AlO$_x$	20.59	16.51	26.78	12.22	16.49

Figure S6. Reverse and forward *J-V* curves and hysteresis index (HI) of freshly prepared ZnO, ZnO/AlO$_x$, ZnO:Al and ZnO:Al/AlO$_x$ based PSCs.

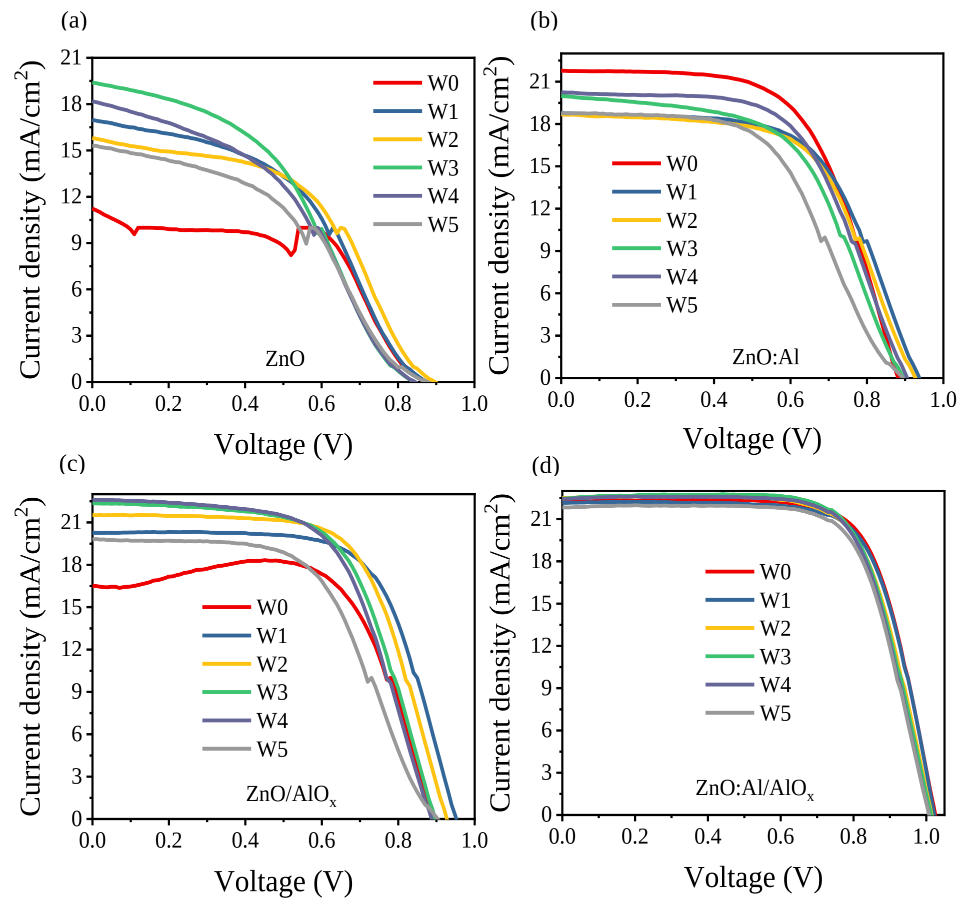

Figure S7. *J-V* curves of 5 freshly prepared perovskite solar cell samples for each type of ZnO: (a) ZnO, (b) ZnO:Al, (c) ZnO/AlO_x and (d) ZnO:Al/AlO_x modified films.

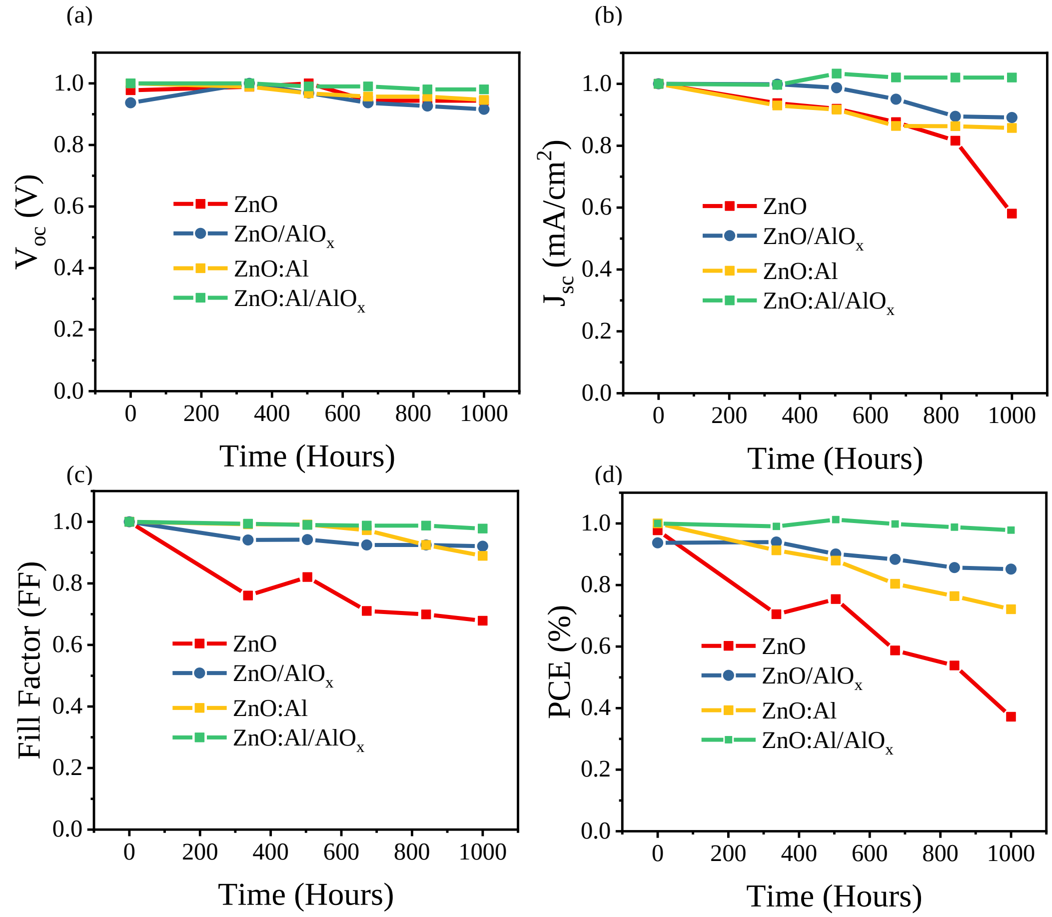

Figure S8. Photovoltaic parameters of ZnO, ZnO:Al, ZnO/AlO$_x$ and ZnO:Al/AlO$_x$ based PSCs as a function of shelf life time (storage time) in ambient conditions.

References:

(S1) Schroder, D.K. Semiconductor Material and Device Characterization, Wiley & Sons, 3, **2006**, 585-590.

(S2) Kwietniewski, N.; Masłyk, M.; Werbowy, A.; Taube, A.; Gierałtowska, S.; Wachnicki, Ł.; Sochacki, M. Electrical characterization of ZnO/4H-SiC n–p heterojunction diode. *Phys. Status Solidi A* **2016**, *213*, 1120–1124.

(S3) Gelderman, K.; Lee, L.; Donne, S. W. Using the Mott–Schottky Equation: Using the Mott–Schottky Equation. *J. Chem. Educ.* **2007**, *84*, 685.

(S4) Alexander, T. P.; Bukowski, T. J.; Uhlmann, D. R.; Teowee, G.; McCarthy, K. C.; Dawley, J.; Zelinski, B. J. J. Dielectric Properties of Sol-Gel Derived ZnO Thin Films. In

ISAF '96. Proceedings of the Tenth IEEE International Symposium on Applications of Ferroelectrics; IEEE, **1996**, 2, 585–588.

(S5) Crisler, D. F.; Cupal, J. J.; Moore, A. R. Dielectric, Piezoelectric, and Electromechanical Coupling Constants of Zinc Oxide Crystals. *Proc. IEEE* **1968**, *56*, 225–226.

(S6) Langton, N. H.; Matthews, D. The Dielectric Constant of Zinc Oxide over a Range of Frequencies. *Br. J. Appl. Phys.* **1958**, *9*, 453–456.

(S7) Lee J. W.; Kim S. G.; Bae S. H.; Lee D. K.; Lin O.; Yang Y.; Park N. G. the interplay between trap density and hysteresis in planar heterojunction perovskite solar cells. *Nano Lett.* **2017**, *17*, 4270−4276.